Spin-Transition and Ferromagnetic Interactions in Copper(II) Complexes of a 3-Pyridyl-Substituted Imino Nitroxide. Dependence of the Magnetic Properties upon Crystal Packing

Fabrice Lanfranc de Panthou,[†] Dominique Luneau,[†] Ryza Musin,[‡] Lars Öhrström,*[,†,⊥] André Grand,[†] P. Turek,[§] and Paul Rey*[,†]

CEA/Département de Recherche Fondamentale sur la Matière Condensée, CNRS/Laboratoire de Chimie de Coordination (URA 1194) SCIB, Centre d'Etudes Nucléaires de Grenoble, F-38054 Grenoble Cedex 9, France, Institut Charles Sadron, 6 Rue Boussingault, 67083 Strasbourg, France, and Institute of Chemical Kinetics and Combustion, Laboratory of Theoretical Chemistry, Russian Academy of Sciences, Siberian Branch, 630090 Novosibirsk, Russia

Received October 9, 1995[⊗]

2-(3-Pyridyl)-4,4,5,5-tetramethyl-4,5-dihydro-1*H*-imidazolyl-1-oxy, IM-3Py (**1**), reacts with copper(II) bis(hexafluoroacetylacetonate), $Cu(hfac)_2$, to give three complexes. One of them is a centrosymmetric three-spin species, $Cu(hfac)_2(IM\text{-}3Py)_2$ (**4**), where two nitroxide ligands are pyridyl bound to the metal and the spins independent from 300 to 5 K. The two other complexes, $[Cu(hfac)_2]_4(IM\text{-}3Py)_2$ (α-phases, **5**, and *β*-phases, **6**) are six-spin clusters comprising four copper(II) ions linked by two tridentate IM-3Py units. Their molecular structures are almost identical, but they crystallize in different space groups. For both complexes, two octahedral *endo* metal ions are involved in a cyclic structure and the two others are *exo*cyclic in a trigonal-bipyramidal environment. On the one hand, the magnetic properties of these two clusters are similar since, for both, the high-temperature behavior can only be accounted for by large ferromagnetic interactions; on the other hand they are dramatically different because the α-phase has a $S = 3$ ground spin state, while the *β*-phase exhibits two transitions resulting in two independent spins below 70 K. The transition temperatures are $T_{C1\uparrow} = 211$ K, $T_{C1\downarrow} = 152$ K, $T_{C2\uparrow} = 80$ K, and $T_{C2\downarrow} = 70$ K. With the help of *ab initio* calculations on model fragments, the presence of a ferromagnetic interaction through the pyridyl ring has been tentatively rationalized invoking McConnell's electron transfer mechanism. The high-temperature transition has been assigned to a change of the *N*-imino coordination from equatorial in a trigonal-pyramidal coordination to axial in a square-planar pyramidal environment at the *exocyclic* copper center. The low-temperature transition corresponds to a switch from axial to equatorial of the nitroxyl coordination at the *endocyclic* octahedral metal ion. Relevant crystallographic parameters are as follows: **4**, triclinic, $P\bar{1}$, a (Å) = 6.955(2), b (Å) = 11.485(2), c (Å) = 14.012(3), α (deg) = 112.55(1), β (deg) = 98.79(1), γ (deg) = 90.28(1), $Z = 1$; **5**, monoclinic, C2/*c*, a (Å) = 25.319(4), b (Å) = 17.653(3), c (Å) = 19.973(4), β (deg) =96.60(2), $Z = 4$; **6**, triclinic, $P\bar{1}$, a (Å) = 12.200(2), b (Å) = 13.389(3), c (Å) = 15.457(3), α (deg) = 102.54(2), β (deg) = 110.16(2), γ (deg) = 92.57(2), $Z = 1$.

Introduction

The design and synthesis of molecular based magnetic materials continue to attract considerable interest.[1−4] One popular strategy in this respect is to combine nitroxide-type radicals with transition metal ions.[5,6] This has so far produced a number of interesting species such as high-spin clusters,[7] ferromagnetic chains,[8] and compounds showing spontaneous magnetization at low temperatures.[9]

Recently we have focused on the preparation of complexes using nitronyl- and imino−nitroxide ligands with three or more possible metal binding sites in order to increase the dimensionality of the systems.[10−12] Two candidates in this respect were the 3-pyridyl-substituted imino nitroxide **1** and its nitronyl nitroxide analogue **2** (Chart 1).

In this contribution we report on the copper(II) bis(hexafluoroacetylacetonato), $[Cu(hfac)_2]$ derivatives of 2-(3-pyridyl)-4,4,5,5-tetramethyl-4,5-dihydro-1*H*-imidazolyl-1-oxy, IM-3Py, (**1**). These complexes include one $S = 3$ ferromagnetic coupled cluster, a two-step spin-transition compound showing hysteresis and one mononuclear complex with three independent $S = 1/2$ spins. Their structures and magnetic properties are presented together with additional first principles quantum chemical calculations on selected model systems.

[†] Centre d'Etudes Nucléaires de Grenoble.
[‡] Russian Academy of Sciences.
[§] Institut Charles Sadron.
[⊥] Present address: Department of Inorganic Chemistry, Chalmers University of Technology, S-412 96 Göteborg, Sweden.
[⊗] Abstract published in *Advance ACS Abstracts,* May 1, 1996.

(1) Day, P. *Science* **1993**, *261*, 431.
(2) Miller, J. S.; Epstein, A. J. *Angew. Chem., Int. Ed. Engl.* **1994**, *33*, 385.
(3) Kahn, O. *Comments Condens. Matter Phys.* **1994**, *17*, 39.
(4) *Localized and Itinerant Molecular Magnetism-From Molecular Assemblies to the Devices*; Coronado, E., Delhaes, P., Gatteschi, D., Miller, J. S., Eds.; NATO ASI; Plenum: New York, in press.
(5) Caneschi, A.; Gatteschi, D.; Sessoli, R.; Rey, P. *Acc. Chem. Res.* **1989**, *22*, 392.
(6) Caneschi, A.; Gatteschi, D.; Rey, P. *Progr. Inorg. Chem.* **1991**, *39*, 331.
(7) Caneschi, A.; Gatteschi, D.; Laugier, J.; Rey, P.; Sessoli, R.; Zanchini, C. *J. Am. Chem. Soc.* **1988**, *110*, 2795.
(8) Cabello, C. I.; Caneschi, A.; Carlin, R. L.; Gatteschi, D.; Rey, P.; Sessoli, R. *Inorg. Chem.* **1990**, *29*, 2582.
(9) Caneschi, A.; Gatteschi, D.; Renard, J. P.; Rey, P.; Sessoli, R. *Inorg. Chem.* **1989**, *28*, 2940.
(10) Caneschi, A.; Ferraro, F.; Gatteschi, D.; Rey, P.; Sessoli, R. *Inorg. Chem.* **1990**, *29*, 4217.
(11) Caneschi, A.; Ferraro, F.; Gatteschi, D.; Rey, P.; Sessoli, R. *Inorg. Chem.* **1990**, *29*, 1756.
(12) Luneau, D.; Risoan, G.; Rey, P.; Grand, A.; Caneschi, A.; Gatteschi, D.; Laugier, J. *Inorg. Chem.* **1993**, *32*, 5616.

S0020-1669(95)01295-X CCC: $12.00

Chart 1

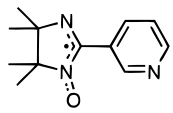

1, IM-3Py

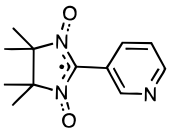

2, NIT-3Py

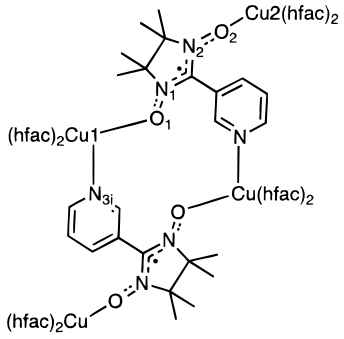

3

The results are discussed and compared to the recently reported copper(II) derivative of the nitronyl nitroxide analogue $[Cu(hfac)_2]_4(NIT\text{-}3Py)_2$, **3**, which also exhibits spin transition but differences in magnetic behavior.[13]

Experimental Section

Syntheses. All reagents and solvents were purchased from commercial sources and used without further purification unless otherwise stated. IM-3Py and $Cu(hfac)_2$ were prepared according to previously reported procedures.[14,15]

$Cu(hfac)_2(IM\text{-}3Py)_2$, 4. Bis[2-(3-pyridyl)-4,4,5,5-tetramethyl-4,5-dihydro-1*H*-imidazolyl-1-oxy]bis(hexafluoroacetylacetonato)copper-(II). IM-3Py (218 mg, 1 mmol) was dissolved in 5 mL of methanol (red solution). A solution of $Cu(hfac)_2$ (239 mg, 0.5 mmol) in hot methanol (30 mL) was then added. The resulting solution was protected from light and left to evaporate at room temperature. After a few days orange needle-shaped crystals of $Cu(hfac)_2(IM\text{-}3Py)_2$ (300 mg, 67%, mp 215 °C) were removed by filtration. Anal. Calcd for $C_{34}H_{34}N_6O_6F_{12}Cu$: C, 44.65; H, 3.75; F, 24.95; N, 9.20; Cu, 6.95. Found: C, 45.12; H, 3.85; F, 24.77; N, 9.25; Cu, 6.96.

α-$[Cu(hfac)_2]_4(IM\text{-}3Py)_2$, 5. α-Bis[2-(3-pyridyl)-4,4,5,5-tetramethyl-4,5-dihydro-1*H*-imidazolyl-1-oxy]tetrakis{[bis(hexafluoroacetylacetonato)]copper(II)}. $Cu(hfac)_2$ (239 mg, 0.5 mmol) was dissolved in 20 mL of heptane and heated to 50 °C. A solution of IM-3Py (54.5 mg, 0.25 mmol) in a minimal amount of dichloromethane was then added to give a dark green solution which was filtered, protected from light, and left at room temperature. After a few days, dark green rhombic crystals of α-$[Cu(hfac)_2]_4(IM\text{-}3Py)_2$ (157 mg, 64%, mp 111 °C) were removed by filtration and washed with pentane. Anal. Calcd for $C_{32}H_{20}N_3O_9F_{24}Cu_2$: C, 32.73; H, 1.72; F, 38.86; N, 3.58; Cu, 10.83. Found: C, 32.69; H, 1.74; F, 38.97; N, 3.65; Cu, 10.80.

***β*-$[Cu(hfac)_2]_4(IM\text{-}3Py)_2$, 6. *β*-Bis[2-(3-pyridyl)-4,4,5,5-tetramethyl-4,5-dihydro-1*H*-imidazolyl-1-oxy]tetrakis{[bis(hexafluoroacetylacetonato)copper(II)}.** This preparation was performed identically to that of **5** except that the solution was left for 3 days in a freezer. A precipitate of **4**, **5**, and **6** was obtained. After filtration needle- or flake-like crystals of *β*-$[Cu(hfac)_2]_4(IM\text{-}3Py)_2$ (17 mg, 7%, mp 101 °C) were separated by manual selection. Anal. Calcd for $C_{32}H_{20}N_3O_9F_{24}Cu_2$: C, 32.73; H, 1.72; F, 38.86; N, 3.58; Cu, 10.83. Found: C, 32.69; H, 1.81; F, 39.03; N, 3.72; Cu, 10.85.

The procedures described above afford crystals suitable for X-ray diffraction studies for all compounds.

X-ray Crystal Structure Analysis. Preliminary Weissenberg photographs showed the triclinic system for **4** and **6** and the monoclinic system (*C*2/*c* space group) for **5**. The intensity data were collected on an Enraf-Nonius CAD4 four-circle diffractometer equipped with Mo Kα radiation and a graphite monochromator using crystals of approximate dimensions 0.2 × 0.2 × 0.2 mm³. Cell constants were derived from a least-squares fit of the setting angles for 25 selected reflections with $10° \le \theta \le 15°$. Crystal structure data are summarized in Table 1. The intensities were corrected for Lorentz and polarization effects but not for absorption.

Table 1. Crystallographic Data for Compounds **4**−**6**

	4	**5**	**6**
formula	$C_{34}H_{34}F_{12}N_6O_6Cu$	$C_{64}H_{40}F_{48}N_6O_{18}Cu_4$	$C_{64}H_{40}F_{48}N_6O_{18}Cu_4$
fw	914.2	2347.17	2347.17
temp (K)	293	293	293
cryst syst	triclinic	monoclinic	triclinic
space group	$P\bar{1}$	*C*2/*c*	$P\bar{1}$
Z	1	4	1
a (Å)	6.955(2)	25.319(4)	12.200(2)
b (Å)	11.485(2)	17.653(3)	13.389(3)
c (Å)	14.012(3)	19.976(4)	15.457(3)
α (deg)	112.55(1)	90	102.54(2)
β (deg)	98.79(1)	96.60(2)	110.16(2)
γ (deg)	90.28(1)	90	92.57(2)
V (Å^3)	1019.06	8867.9	2293.8
ρ (g·cm^{-3})	1.49	1.76	1.69
μ(Mo Kα) (cm^{-1})	15.89	15.42	15.42
R^a	0.064	0.083	0.070
$R_w{}^b$	0.078	0.096	0.068

[a] $R = \sum||F_o| - |F_c||/\sum|F_o|$. [b] $R_w = (\sum w(|F_o| - |F_c|)^2/\sum w|F_o|^2)^{1/2}$. $w = 1/\sigma F_o^2$.

Table 2. Selected Bond Lengths (Å) and Angles (deg) for **4**−**6**

	4	**5**	**6**
Cu1−O1		2.640(5)	2.599(4)
Cu1−O2	1.969(4)	1.936(3)	1.943(4)
Cu1−O3	2.272(3)	1.961(4)	1.976(5)
Cu1−O4		2.214(5)	2.171(6)
Cu1−O5		1.936(3)	1.932(4)
Cu1−N3	2.049(3)	2.010(4)	2.013(5)
Cu2−O6		2.019(5)	2.067(6)
Cu2−O7		1.910(5)	1.928(4)
Cu2−O8		1.926(5)	1.891(6)
Cu2−O9		2.048(6)	2.011(6)
Cu2−N2		2.044(6)	2.017(6)
O1−N1	1.245(5)	1.281(7)	1.263(6)
O1−Cu1−O4		167.0(2)	175.9(2)
O1−Cu1−N3		83.5(2)	80.4(2)
O2−Cu1−O5		173.8(2)	175.7(2)
O3−Cu1−N3		165.7(2)	171.0(2)
O6−Cu2−O9		109.4(3)	97.7(3)
O6−Cu2−N2		127.0(2)	122.9(2)
O7−Cu2−O8		178.3(2)	174.9(2)
O9−Cu2−N2		123.6(3)	139.4(2)

[a] For compound **4**, Cu1 stands for the unique copper ion.

For **4** and **6,** the initial choice of the $P\bar{1}$ space group was fully confirmed by all developments during structure determination using the SHELX86 and SHELX76 packages.[16] The Cu(II) ion positions were obtained from Patterson maps. The remaining non-hydrogen atoms were located in a succession of difference Fourier syntheses and were least-squares refined with anisotropic thermal parameters. For **5** and **6**, some CF_3 groups were disordered and, considering Fourier difference maps, were modeled including six fluorine positions with half-occupancy. The hydrogen atoms were included in the final refinement models in calculated and fixed positions with isotropic thermal parameters.

Selected bond lengths and angles are listed in Table 2. Summaries of crystal data (Table S1), positional parameters (Tables S2−S4), calculated positions of hydrogen atoms (Tables S5−S7), complete listing of bond lengths (Tables S8−S10), bond angles (Tables S11−S13), and anisotropic thermal parameters (Tables S14−S16) are deposited as Supporting Information.

(13) Lanfranc de Panthou, F.; Belorizky, E.; Calemczuk, R.; Luneau, D.; Marcenat, C.; Ressouche, E.; Turek, P.; Rey, P. *J. Am. Chem. Soc,* **1995**, *117*, 11247.
(14) Ullman, E. F.; Call, L.; Osiecki, J. H. *J. Org. Chem.* **1970**, *35*, 3623.
(15) Belford, R. L.; Martell, A. E.; Calvin, M. *J. Inorg. Nucl. Chem.* **1956**, *2*, 11.
(16) Sheldrick, G. M. SHELLX86 In *Crystallographic Computing 3*; Sheldrick, G. M., Kruger, C., Goddard, R., Eds; Oxford University Press: Oxford, U.K., 1985; p 175; *SHELX76 System of Computing Programs*; University of Cambridge: Cambridge, England, 1976.

Magnetic and EPR Measurements. Magnetic susceptibility data were measured on the bulk material, in the 2−300 K temperature range, with a Quantum Design MPMS superconducting SQUID magnetometer operating at a field strength of 0.5 T. The crude squid outputs were corrected for the magnetization of the sample holder, and the magnetic susceptibilities were corrected for the diamagnetism of the constituent atoms using Pascal constants.

EPR experiments were performed on a Bruker ER-200 spectrometer operating at 9.3 MHz. The TE102 cavity was equipped with an Oxford continuous-flow cryostat and a thermocouple for low-temperature data recording.

Computational Details. Two methods of computation were used: density functional theory (DFT) and restricted open-shell Hartree−Fock (ROHF) combined with a 3 × 3 configuration interaction (CI) using the magnetic orbitals.

DFT computations were performed with the DGauss 2.3 program,[17] including the VWN functional[18] at the local spin density level. For the nonlocal corrections to the exchange-correlation energy, the Becke−Perdew (BP) functional,[19] including a gradient corrected exchange, was used in a perturbative way on the LSD SCF density.[20]

All geometries were taken from the X-ray diffraction determinations and hydrogens positioned by standard bond lengths and angles. The CF_3 groups on the hexafluoroacetylacetonato ligands were replaced by hydrogen atoms (new ligand abbreviated *pb*) in all cases except for one reference calculation. All calculations were made on the high-spin state of the respective model compounds.

Restricted open-shell Hartree−Fock calculations were done with the Gaussian-92 program.[21] Calculations of the coupling constants, *J*, were done with a 3 × 3 CI, as described previously.[22]

Results

The reaction of $Cu(hfac)_2$ and IM-3Py gave three different compounds which have been fully characterized by X-ray structure determination and magnetic susceptibility measurements. We will first report on the structural and magnetic properties and then follow up with complementary quantum chemical calculations.

Structural Studies. (a) $Cu(hfac)_2(IM\text{-}3Py)_2$, 4. The copper(II) ion is located on an inversion center, and as seen in Figure 1, the metal environment is octahedral with a Jahn−Teller elongation of about 0.2 Å along one O−Cu−O axis, the pyridyl nitrogens being equatorially bound. All L−Cu−L angles are close to 90°, and the angle between the two cyclic fragments of the IM-3Py unit is 27.3°. The closest intermolecular contacts (O1−N′2 = 4.6 Å, O1−O′1 = 4.9 Å) between uncoordinated nitroxyl and/or imino groups are not expected to mediate strong exchange interactions.

(b) α-$[Cu(hfac)_2]_4(IM\text{-}3Py)_2$, 5. The molecular unit comprises four $Cu(hfac)_2$ and two IM-3Py fragments symmetry related by an inversion center (Figure 2). Two $Cu(hfac)_2$ (Cu1) and two IM-3Py units form a ring where the copper ions are in a distorted octahedral environment with one long axial Cu1−nitroxide(oxygen) bond (2.640(5) Å) and one equatorial Cu1−pyridyl bond (2.010(4) Å). The other largest deviation from an ideal octahedral pattern is found for the N(pyridyl)−Cu−O(nitroxyl) angle (83.5(2)°). The remaining imino ligating site of the nitroxide ligands occupies an equatorial position in the five-coordinated trigonal-bipyramidal Cu2 unit (Cu2−N2 = 2.044(6) Å). The five- and six-membered rings of the IM-3Py unit make an angle of 49.2°.

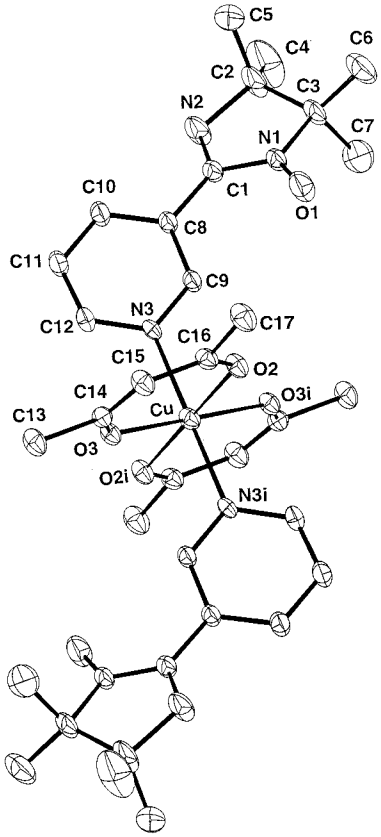

Figure 1. View of the molecular structure of $Cu(hfac)_2(IM\text{-}3Py)_2$, **4**. Fluorine atoms have been omitted for the sake of clarity. Thermal ellipsoids are drawn at the 30% probability level. i's indicate atoms related by the symmetry: $-x, -y, -z$.

The shortest intermolecular Cu−Cu distances are 7.67 Å (Cu2−Cu′2) and 10.08 Å (Cu1−Cu′1).

(c) β-$[Cu(hfac)_2]_4(IM\text{-}3Py)_2$, 6. The molecular unit is almost identical to that of the α-phase **5** (Figure 3). Significant differences are however found for the environment of the *exo*cyclic Cu2 ions. In **6**, this part deviates notably from ideality in the basal plane, where the three angles are different and far from the ideal value of 120° (O9−Cu2−N2 = 139.4(2)°), and in slight nonlinearity of the axial atoms, O7−Cu2−O8 = 174.9-(2)°. Significantly different are also the angles between the metal equatorial planes and the five- and six-membered rings of the nitroxide ligand, respectively. In **5** these angles are 31.8 and 11.9°, while the corresponding values in **6** are 38.0 and 16.0°.

The major difference, however, is found in crystal packing and intermolecular parameters (see Discussion), which are the consequence of different space groups. The closest intermolecular contacts between spin carriers are Cu2−Cu′2 (7.96 Å) and Cu1−Cu′1 (8.86 Å).

Magnetic Properties. (a) $Cu(hfac)_2(IM\text{-}3Py)_2$. Magnetic data for **4** are reported in Figure 4 as χT vs T. The Curie law

(17) Andzelm, J.; Wimmer, E. *J. Chem. Phys.* **1992**, *96*, 1280 (included in the *UniChem 2.3* package from Cray Research, Inc., Mendota, Heights, MN, 1994). The Dgauss program uses Gaussian basis sets optimized for DFT calculations. A double ζ split-valence plus polarization basis set, DZVP, was used. Contracted basis sets were taken from: Godbout, N.; Salahub, D. R.; Andzelm, J.; Wimmer, E. *Can. J. Chem.* **1992**, *70*, 560.

(18) Vosko, S. H.; Wilk, L.; Nusair, M. *Can. J. Phys.* **1980**, *58*, 1200.

(19) Becke, A. D. In *The Challenge of d and f Electron*; Salahub, D. R., Zerner, M. C., Eds.; ACS Symposium Series 394; American Chemical Society; Washington, D.C., 1989; p 166 and references cited therein.

(20) In some cases the nonlocal corrections were included self-consistently. This procedure was time consuming, and the spin populations and orbital energies did not show significant differences from the LSD calculations.

(21) Frisch, M. J.; Trucks, G. W.; Head-Gordon, M.; Gill, P. M. W.; Wong, M. W.; Foresman, J. B.; Johnson, B. G.; Schlegel, H. B.; Robb, M. A.; Replogle, E. S.; Gomperts, R.; Andres, J. L.; Raghavachari, K.; Binkley, J. S.; Gonzales, C.; Martin, R. L.; Fox, D. J.; Defrees, D. J.; Baker, J.; Stewart, J. J. P.; Pople, J. A. *Gaussian 92*, Revision G.2; Gaussian, Inc.: Pittsburgh, PA, 1992.

(22) Ovcharenko, V. I.; Romanenko, G. V.; Ikorskii, V. N.; Musin, R. N.; Sagdeev, R. Z. *Inorg. Chem.* **1994**, *33*, 3370.

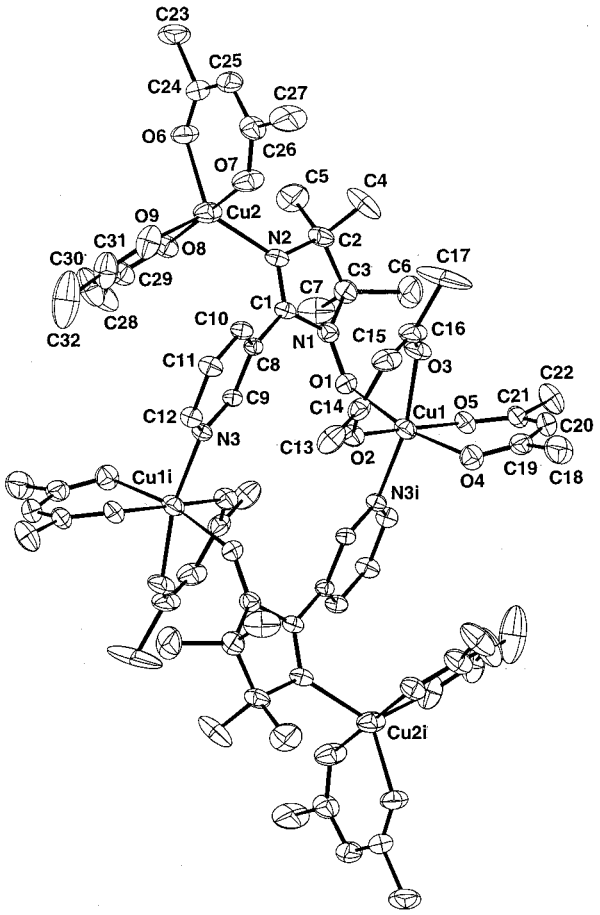

Figure 2. View of the molecular structure of α-[Cu(hfac)$_2$]$_4$(IM-3Py)$_2$, **5**. Fluorine atoms have been omitted for the sake of clarity. Thermal ellipsoids are drawn at the 30% probability level. i's indicate atoms related by the symmetry: $^1/_2 - x$, $^1/_2 - y$, $-z$.

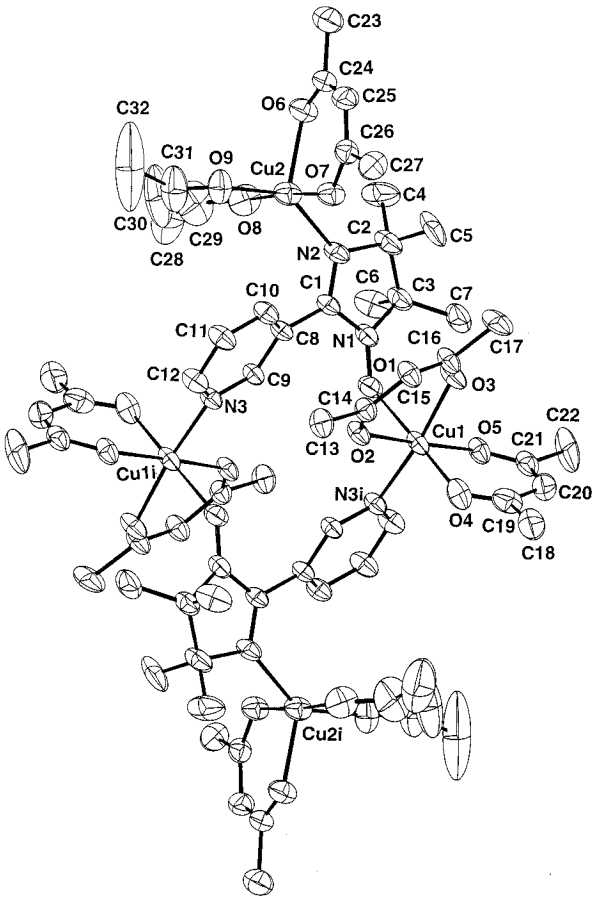

Figure 3. View of the molecular structure of β-[Cu(hfac)$_2$]$_4$(IM-3Py)$_2$, **6**. Fluorine atoms have been omitted for the sake of clarity. Thermal ellipsoids are drawn at the 30% probability level. i's indicate atoms related by the symmetry: $1 - x$, $1 - y$, $-z$.

Chart 2

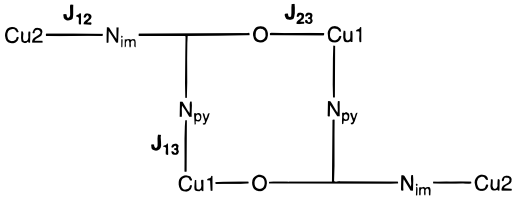

behavior with χT = 1.25 emu K mol^{-1} (3.16 μ_B), which corresponds to three independent spins $s = ^1/_2$, shows that intra- and intermolecular interactions are weak and are not operative within the 5−300 K temperature range.

(b) α-[Cu(hfac)$_2$]$_4$(IM-3Py)$_2$. Magnetic data for **5** are displayed in Figure 5 as χT vs T. At room temperature the value of χT = 2.97 emu K mol^{-1} (4.87 μ_B) is much larger than that expected for six independent spins $S = ^1/_2$ (χT = 2.25 emu K mol^{-1} if $g = 2$) but corresponds well to two spins $S = 1$ and two spins $S = 1/2$ (χT = 2.97 emu K mol^{-1}, g = 2.08). At 2 K, χT reaches a value of 5.68 emu K mol^{-1} (6.8 μ_B), which is close to the theoretical value for $S = 3$, χT = 6.0 emu K mol^{-1}.

Considering the centrosymmetric molecular structure and the large intermolecular distances between spin carriers, the magnetic behavior was fit against a model involving three independent coupling constants between bound spin carriers (Chart 2). Numerical diagonalization of the isotropic spin Hamiltonian ($H = -2J_{ij}S_iS_j$)[23] gave the following best fit values: 213(12),

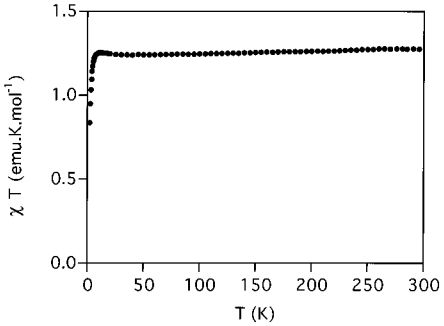

Figure 4. Temperature dependence of the product of the magnetic susceptibility with temperature, χT vs T, for Cu(hfac)$_2$(IM-3Py)$_2$, **4**.

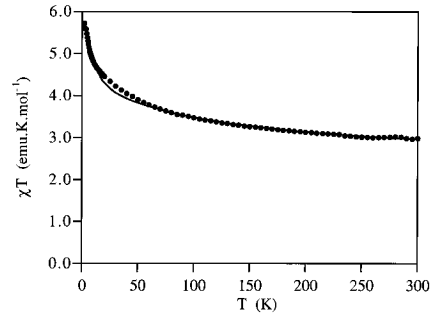

Figure 5. Temperature dependence of the product of the magnetic susceptibility with temperature, χT vs T, for α-[Cu(hfac)$_2$]$_4$(IM-3Py)$_2$, **5**. The solid line is calculated with the parameters reported in the text.

(23) Belorizky, E.; Fries, P. H.; Gojon, E.; Latour, J.-M. *Mol. Phys.* **1987**, *61*, 661.

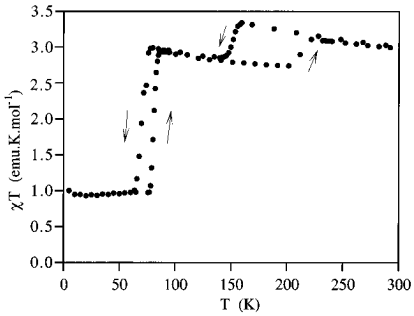

Figure 6. Temperature dependence of the product of the magnetic susceptibility with temperature, χT vs T, for β-$[Cu(hfac)_2]_4(IM\text{-}3Py)_2$, **6**.

93(4), and 5.5(9) cm^{-1} with $g = 2.065$. A model involving two spins $S = 1$ and two spins $S = {}^1/_2$ gave almost identical results for the two smaller coupling constants, and introduction of parameters describing exchange interactions between nonbonded spin carriers gave no additional information.

(c) β-$[Cu(hfac)_2]_4(IM\text{-}3Py)_2$, 6. This molecule, almost identical to **5**, proved to have dramatically different magnetic properties as shown in Figure 6, where the temperature dependence of χT is displayed. At room temperature the value of χT (3.00 emu K mol^{-1}, 4.9 μ_B) is much larger than the value expected for six independent spins $S = {}^1/_2$ ($\chi T = 2.25$ emu K mol^{-1}) but, as for **5**, corresponds well to two spins $S = 1$ and two spins $S = 1/2$ ($\chi T = 2.97$ emu K mol^{-1}). The following increase in χT when the temperature is decreased to 160 K parallels that observed for compound **5** in the same temperature range. Owing to the similar molecular structures and similar magnetic behaviors, these high-temperature data were fit against the same model (Chart 2). However, considering the low number of data, a model taking into account only two spins $S = 1$ and two spins $S = {}^1/_2$ was used which afforded coupling constants of 82(11) and 7(2) cm^{-1}.

At 150 and 70 K one observes two abrupt drops in χT from 3.42 to 2.80 emu K mol^{-1} (4.73 μ_B) and then from 3.03 to 0.95 emu K mol^{-1} (2.75 μ_B). This latter value corresponds well to two independent spins $S = {}^1/_2$, and from this point we observe a Curie law behavior. Both transitions occur with hysteresis, and the transition temperatures are $T_{C1\uparrow} = 211$ K, $T_{C1\downarrow} = 152$ K, $T_{C2\uparrow} = 80$ K, and $T_{C2\downarrow} = 70$ K. No change in transition temperatures was noticed when a sample was cooled and warmed several times, nor when the data were collected at different field strengths. It is worth noting that below 200 K the crystals broke into a very thin powder such that a low-temperature structure determination could not be attempted.

Compounds **5** and **6** are EPR silent at room temperature, as observed previously for several copper(II) nitroxide clusters.[13] At low temperature, the spectra exhibit many broad features which do not allow any interpretation but strongly suggest that at 4.2 K spin states larger than ${}^1/_2$ are thermally populated.

Quantum Chemical Calculations. Recent calculations have shown that DFT affords spin densities in good agreement with experiment for a number of organic radicals.[24] Since the spin density is closely related to the magnetic couplings,[25] and also because DFT can handle large systems, this method was chosen. In addition, a 3 × 3 CI approach with wave functions from ROHF calculations, recently used with some success to calculate the coupling constants J for metal−nitroxide complexes,[22] was attempted.

The target of these calculations was the understanding of the ferromagnetic couplings in **5**. Since in related compound **3** these interactions are absent but the structure is similar, models for this complex were also included in the investigation. Furthermore, in order to test the robustness of the method and the errors introduced by the simplification of the ligands, a number of reference calculations were made.[26] The most important conclusion was that the omission of the CF_3 groups caused, as expected, a destabilization of the d orbitals (∼1 eV); *changes* in orbital energies were, however, consistent as well as the spin populations and orbital interactions. Table 3 shows a comparison of the properties of the imino and the nitronyl nitroxide radical models shown in Chart 3.

On considering the molecular structures of **3**−**5**, it was thought that the ligation of several metal units to the IM-3Py ligand was perturbating the spin density distribution in the radical. To test this assumption, computations of some bimetallic units of the α-$[Cu(hfac)_2]_4(IM\text{-}3Py)_2$ molecule **5** were performed. However, the orbital interactions and spin populations in $[Cu_{endo}(pb)_2]_2[N_{py},O\text{-}(IM\text{-}3Py^{**})]_2$, $[Cu_{endo}(pb)_2]N_{im},O\text{-}(IM\text{-}3Py^{**})[Cu_{exo}(pb)_2]$, and $[Cu_{endo}(pb)_2]N_{im},N_{py},\text{-}(IM\text{-}3Py^{**})\text{-}[Cu_{exo}(pb)_2]$ showed no significant differences from corresponding smaller models comprising only one copper(II) ion.

We then investigated the bonding to each potential coordination site in IM-3Py in more detail; relevant orbital energies and spin populations of $Cu_{endo}(pb)_2(O\text{-}IM^*)(py)$, **7** (Chart 4), and $Cu_{exo}(pb)_2(N_{im}\text{-}IM^*)$, **8**, are found in Table 3.

Finally, the coupling constants J ($H = -2JS_AS_B$) for the fragments **7**, **8**, and $Cu_{endo}(pb)_2(O\text{-}ONH_2)(N_{py}\text{-}IMpy^*)$, **10**, were calculated with the 3 × 3 CI approach, and the values are reported in Table 4. The agreement with experimental values is only qualitative since, as mentioned, the replacement of the CF_3 groups by hydrogen atoms destabilizes the d-orbitals. This means that the energy difference to the NO π^* orbitals will decrease and consequently the orbital mixing will increase. This fact is especially important in **9** since a very small d_{z^2} NO π^* overlap is given unproportional weight (anitiferromagnetic contribution) by a quasi-degeneracy of the orbitals.

Discussion

The coordination properties of pyridyl substituted nitronyl and imino nitroxides were investigated because, thanks to the presence of three sites of coordination, complexes of high dimensionality were expected. Although all of the derivatives of these ligands are discrete, they are often polynuclear and they exhibit interesting magnetic features. In the case of the copper derivatives of the *m*-pyridyl nitroxides **4**−**6**, one observes large ferromagnetic interactions and a spin-transition behavior which are unprecedented in the magnetochemistry of nitroxide−metal complexes.

$Cu(hfac)_2(IM\text{-}3Py)_2$, 4. In this three-spin system the only realistic coupling pathway would involve spin-polarization of the pyridyl nitrogen. Such a mechanism has been considered

(24) (a) Zheludev, A.; Bonnet, M.; Delley, B.; Grand, A.; Luneau, D.; Öhrström, L.; Ressouche, E.; Rey, P.; Schweizer, J. *J. Magn. Magn. Mater.* **1995**, *145*, 293. (b) Zheludev, A.; Grand, A.; Ressouche, E.; Schweizer, J.; Morin, B. G.; Epstein, A. J.; Dixon, D. A.; Miller, J. S. *Angew. Chem., Int. Ed. Engl.* **1994**, *33*, 1379. (c) Zheludev, A.; Barone, V.; Bonnet, M.; Delley, B.; Grand, A.; Ressouche, E.; Rey, P.; Subra, R.; Schweizer, J. *J. Am. Chem. Soc.* **1994**, *116*, 2019.

(25) Kahn, O. *Molecular Magnetism*; VCH: Weinheim, Germany, 1993.

(26) The level of theory was increased by performing the nonlocal correction in every SCF step. Triple ζ basis sets were also introduced for both Cu and the lighter elements. Neither of these trials indicated that our method was insufficient. The effect of changing the CF3 groups to hydrogens were probed by performing calculations on imino-coordinated fragments: Cu(hfac)2(IM-3Py**) and Cu(pb)2(IM-3Py**). Changes in spin populations and in the nature of the magnetic orbitals were negligible. Comparison of the fragments IM-3Py, IM-3Py*, IM-3Py**, and NIT-3Py* shows effects on both spin populations and orbital energies, but there are only differences in magnitude and the models all show the same phenomenological behavior.

Table 3. Summary of the Density Functional Theory Calculations[a]

	for given molecule (method; spin state)								
	IM-3Py* (NLSCF; $^1/_2$)	NIT-3Py* (NLSCF; $^1/_2$)	IM* (LSD; $^1/_2$)	NIT* (LSD; $^1/_2$)	**7** (LSD; 1)	**8** (LSD; 1)	**9**[b] (LSD; 1)	**9LT**[c] (LSD; 1)	**9LT**[c] (LSD; 0)
					α-MO's (eV)				
NO p*	*−5.55*	*−4.53*	*−5.93*	*−4.36*	*−4.50*	*−5.40*	*−4.14*	*−4.14*	*−4.67*
$d_{x^2-y^2}$					*−4.44*	*−5.43*	−4.49	*−4.62*	*−4.20*
d_{z^2}					*−4.90*	*−4.68*	*−4.86*	*−4.89*	
					β-MO's (eV)				
NO π*	−4.47	−3.55	−3.95	−3.62	−3.69	−4.56	−3.48	−3.52	
$d_{x^2-y^2}$					−3.38	*−5.20*	−3.86	−4.30	
d_{z^2}					*−4.67*	−4.06	*−4.62*	*−4.37*	
					Spin Population				
Cu					0.484	0.474	0.504	0.532	0
O_{NO}	0.509	0.315	0.468	0.309	0.432	0.470	0.262	0.228	0
N_{NO}	0.283	0.210	0.286	0.200	0.287	0.285	0.197	0.196	0
C	−0.073	−0.092	−0.045	−0.077	−0.044	−0.033	−0.070	−0.049	0
$N_{NO'}$		0.242		0.266			0.218	0.203	0
$O_{NO'}$		0.329		0.325			0.317	0.316	0
N_{imino}	0.262		0.258		0.248	0.264			
$N_{pyridyl}$	0.002	0.003			0.068		0.070	0.095	0
energy[d] (a.u.)								−0.26517	−0.26892

[a] Orbital energies in italics refer to occupied orbitals. [b] Room temperature structure, axial NO. [c] Structure at 50 K, equatorial NO. [d] Total energy, +2799 au.

Chart 3

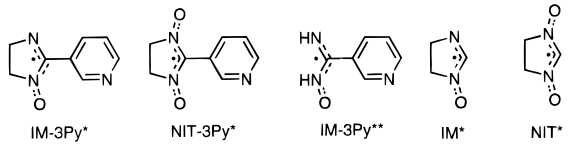

Chart 4

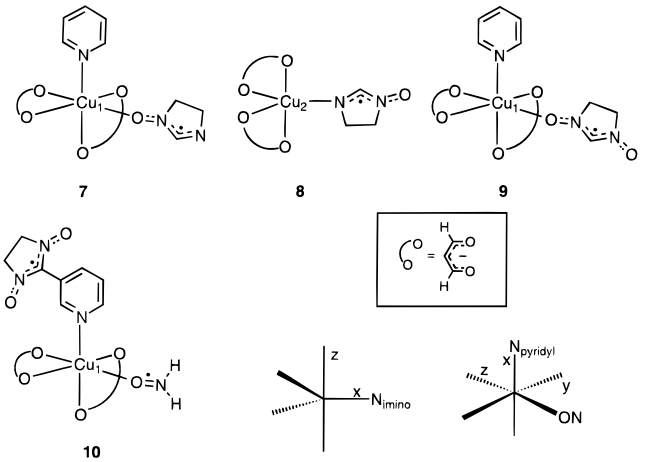

to explain the observed interactions in Mn(II) (+0.5 and −8.6 cm^{-1})[10,27] and Cu(II) (−9.2 cm^{-1})[11] complexes of *p*-pyridyl substituted nitroxides. In contrast, the only known example of a copper derivative of a *m*-pyridyl substituted nitroxide exhibits, as **4**, a Curie behavior down to 4 K.[28] Rationalization of these features is found in Table 3, where the calculated spin density carried by the *m*-pyridyl nitrogen in IM-3Py is much weaker than the corresponding one in the *para*-substituted analogue.

α-[Cu(hfac)$_2$]$_4$ (IM-3Py)$_2$, 5. Considering the weakness of the coupling mediated by the pyridyl group, it was surprising to observe a $S = 3$ ground state described by three ferromagnetic couplings (213, 93, and 5.5 cm^{-1}) in **5**. Assignment of these interactions to specific pathways relies on earlier studies.

Table 4. Relevant ROHF Orbital Energies, Spin Populations, and Magnetic Coupling Constants Calculated by 3 × 3 CI for Model Complexes **7**, **8**, and **10**

	for given molecule (spin state)		
	7[a] (1)	**8** (1)	**10** ($^3/_2$)
MO's (eV)			
NO π*	−3.17	−4.21	−3.16
NO′ π*			−3.55
8, d_{z^2}; **7**, **10**, $d_{x^2-y^2}$	−3.84	−4.06	−3.85
Spin Populations			
Cu	0.943	0.947	0.944
O_{NO}	0.776	0.836	0.777
N_{NO}	0.220	0.123	0.220
C		0.007	0.002
$O_{NO'}$			0.818
$N_{NO'}$			0.142
N_{imino}		0.034	0.028
$N_{pyridyl}$	0.011		0.011
Spin delocalization ρ_i (i = Orbitals)			
8: Cu···N_{imino}---N−•O coordination			
ρ_{π^*} [from Cu(d_{z^2}) to NO(π*)]		0.041	
ρ_{z^2} [from NO(π*) to Cu(d_{z^2})]		0.035	
7, **10**: Cu···O•−N---N_{imino} coordination			
ρ_{π^*} [from Cu($d_{x^2-y^2}$) to NO(π*)]	$<10^{-4}$		$<10^{-4}$
ρ_{z^2} [from NO(π*) to Cu(d_{z^2})]	0.001		0.001
Coupling (cm^{-1})			
J_{Cu-NO}	16.0	9.2	15.5.0
$J_{Cu-NO'}$			<0.1
J_{NO-NO}			<0.01

[a] The smaller fragment, ONH_2 was used instead of IM*.

Indeed, a trinuclear copper derivative of the phenyl substituted ligand has been reported[29] in which both the equatorial imino coordination to a trigonal-bipyramidal copper(II) ion and the axial oxygen coordination to an octahedral metal center occur with similar binding parameters and coupling constants of ca. +200 and +5 cm^{-1}. Therefore, the larger (213 cm^{-1}) and the weaker (5.5 cm^{-1}) calculated parameters were respectively attributed to the *exo*-Cu2−$N_{imino,}$ J_{12}, and to the *endo*-Cu1−O(nitroxyl), J_{23}, interactions (Chart 2). Accordingly, the

(27) Kitano, M.; Ishimaru, Y.; Inoue, K.; Koga, N.; Iwamura, H. *Inorg. Chem.* **1994**, *33*, 6012.
(28) Lanfranc de Panthou, F. Thesis, Centre d'Etudes Nucléaires de Grenoble, 1994.
(29) Luneau, D.; Rey, P.; Laugier, J.; Fries, P.; Caneschi, A.; Gatteschi, D.; Sessoli, R. *J. Am. Chem. Soc.* **1991**, *113*, 1245.

medium interaction (93 cm^{-1}) was assigned to the J_{13} mediated by the pyridyl ring.

Such a large coupling across the pyridyl group could be accounted for by means of orthogonal orbitals[25] or McConnell's spin polarization mechanism[30] only if a large spin density is carried by the nitrogen atom. Since such an interaction is not observed in **4**, the logical origin of a modification of the spin distribution would be that the attachment of the two copper ions to the IM-3Py ligand perturbs the π-system in such a way that a significant delocalization or polarization to the pyridyl ring takes place. However, no sign of a change in spin distribution can be seen in our calculations. To get insight into this problem, it is helpful to look at the differences between the IM-3Py complex **5** and the NIT-3Py analogue **3**. The spin populations on the pyridyl ring do not differ much; indeed, they are even slightly higher in **3**, where no pyridyl mediated interaction is observed. What clearly differs, however, is the behavior of the nitroxide π-orbital energies. Coordination of Cu(II) to the nitroxyl oxygen of IM-3Py and to any of the nitroxyl groups of NIT-3Py destabilizes the NO π^* level somewhat. In contrast, the empty IM-3Py β-π^*-orbital gets 0.6 eV more stable when the imino nitrogen is bound to a copper ion. If this stabilization is the key to the ferromagnetic coupling, we have to invoke McConnell's second mechanism involving electron transfer.[31,32] This mechanism is hard to lead into evidence and, in contrast to the original proposition, may not always lead to a high-spin ground state.[32] A suitable pathway for this electron transfer mechanism would in this case be the transfer of a metal β-d-electron to the stabilized ligand β-π^*-orbital from the *endo*cyclic Cu1 metal center via the pyridyl π-system. This transfer would result in an hexacoordinated Cu(III) species where a high-spin state seems likely,[33] and at the same time the spin information has passed from one half of the molecule to the other. Given the speculative nature of this interpretation, we will not pursue this issue further. Nevertheless it is worth underlining that the π^*-orbital stabilization is the only significant difference between α-$[Cu(hfac)_2]_4(IM\text{-}3Py)_2$ and $[Cu(hfac)_2]_4(NIT\text{-}3Py)_2$ resulting from these calculations.

Finally, it is worth mentioning that the two other interactions are rationalized in the frame of these calculations which agree also with all previously reported experimental studies on imino nitroxides.

***β*-[Cu(hfac)$_2$]$_4$(IM-3Py)$_2$. Spin Transformations.** Recently we reported on the magnetic properties of compound **3**,[13] which exhibits a spin transformation without hysteresis at 110 K and a structure closely related to those of **5** and **6**. Therefore, it was not a surprise to find a similar transition in **6**; to find two in **6** and none in **5** was, however, totally unexpected.

Although a low-temperature structure is not available for **6**, the decrease of χT at 70 K has been ascribed to a switch from axial to equatorial of the nitroxyl oxygen coordination to the *endo*cyclic Cu1 copper ion. Indeed, the same change corresponding to the disappearance of four spins has been experimentally shown to be the consequence of such a switch in **3**. For both compounds, this switch results in a strong antiferromagnetic coupling between the *endo* copper ions and the nitroxide ligands, leading to independent *exo* metal centers at low temperature.[6] Preliminary specific heat data[34] do document an entropy variation consistent with the expected spin multiplicities at low and high temperatures. The presence of hysteresis suggests that the transformation is cooperative in the present case and is related to the presence of intermolecular interactions. The low-temperature EPR spectra bring a qualitative support to this suggestion for they show that in **6** the *exo* copper centers are interacting. These intermolecular interactions are weak because they do not show up in the low-temperature magnetic data.

In contrast, the high-temperature transition does not correspond to a change of spin multiplicity and the weakness of the drop in χT suggests that it results from a change in magnitude of an interaction. Within the 200−300 K temperature range, the magnetic behavior is almost identical to that of **5** and well-described by three ferromagnetic interactions among which one is very large. Considering the magnetic behavior between the two transitions (85 and 205 K), a value of χT at 205 K (2.80 emu K mol^{-1}) lower than that at 300 K (2.97 emu K mol^{-1}) clearly precludes the presence of such a large interaction. Thus, it is inferred that the strong ferromagnetic coupling between the imino nitroxide and the *exo* copper ion (Cu2) has substantially decreased. We attempted a simulation of this magnetic behavior using the same model as that for **5**, but, owing to the limited number of data within the 85−205 K temperature range, J_{13} and J_{23} were assumed not to vary and were fixed to 82 and 7 cm^{-1}, respectively. This model affords a value of J_{12} of 8.5 cm^{-1} and a calculated value of χT at 300 K of 2.58 emu K mol^{-1}, which is close to that of six independent spins $^1/_2$. Since the nitrogen equatorial coordination of imino nitroxides to copper(II) always results in strong ferromagnetic couplings whatever the geometry of the metal environment,[29] the only way to explain a weak ferromagnetic coupling is to consider an axial coordination below 200 K. Considering the magnetic orbitals, in such a situation the imino nitrogen coordination would be similar to that of any nitroxyl oxygen for which weak interactions of ca. +10 cm^{-1} are generally observed independently of the geometry of the metal unit.[35,36] Although the final geometry of the pentacoordinate Cu(2) can be described as a trigonal bipyramid or a square-planar pyramid, the displacement of the atoms involved in both processes is less important in the latter case so that a square-planar pyramid is more likely. Indeed, an angle as large as 139° in the basal plane of Cu2 shows that the room-temperature trigonal-pyramidal geometry is distorted toward a square-pyramidal environment. Therefore, we propose that the high-temperature transition is the consequence of a geometry change from equatorial in a trigonal bipyramid to axial in a square-planar pyramid of the coordinated imino nitrogen at the *exo*cyclic Cu2 ion which shifts the coupling from strongly ferromagnetic to weakly ferromagnetic.

Such a coordination change at the *exo*-Cu2 ion in **6** results for the 85−205 K phase in a structural arrangement similar to that observed in **3**, suggesting that this coordination change is a prerequisite for the low-temperature transition. This suggestion is strongly supported by the magnetic behavior of complex **5** (α-phase) where no transition occurs. Indeed, examination of Figures 7 and 8, in which are represented the crystal packings and particularly the relative arrangements of neighbor Cu2 centers in **5** and **6**, affords an answer for the absence of transition in the α phase. In both phases, intermolecular contacts of ca. 5 Å between carbon atoms of CF3 groups, which bring the

(30) McConnell, H. M. *J. Chem. Phys.* **1963**, *39*, 1916.
(31) McConnell, H. M. *Proc. Robert A. Welch Found. Conf. Chem. Res.* **1967**, *11*, 144 (reproduced an discussed in: Breslow, R. *Pure Appl. Chem.* **1982**, *54*, 927).
(32) Kollmar, C.; Kahn, O. *Acc. Chem. Res.* **1993**, *26*, 259.
(33) Harnischmacher, W.; Hoppe, R. *Angew. Chem., Int. Ed. Engl.* **1973**, *12*, 582.
(34) Calemzuk, R.; Marcenat, C. Personal communication.
(35) Caneschi, A.; Gatteschi, D.; Grand, A.; Laugier, J.; Pardi, L.; Rey, P. *Inorg. Chem.* **1988**, *27*, 1031.
(36) Musin, R. N.; Schastnev, P. V.; Malinkovskaya, S. A. *Inorg. Chem.* **1992**, *31*, 4118.

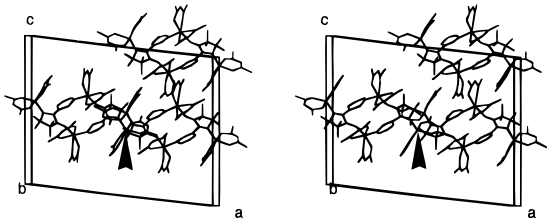

Figure 7. Stereoview showing the crystal packing in α-$[Cu(hfac)_2]_4$-$(IM\text{-}3Py)_2$, **5**. The arrow indicates the position of the *exo*cyclic Cu2 metal center.

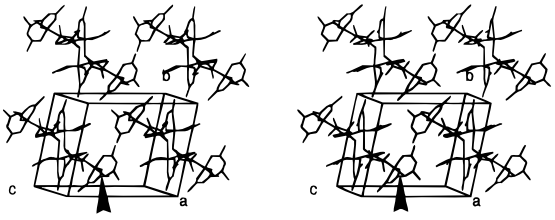

Figure 8. Stereoview showing the crystal packing in β-$[Cu(hfac)_2]_4$-$(IM\text{-}3Py)_2$, **6**. The arrow indicates the position of the *exo*cyclic Cu2 metal center.

fluorine atoms at the limit of the van der Waals radius, are observed. Owing to the different space groups, these metal centers (Cu2) are related by a C_2 axis in **5**, while they are related by an inversion center in **6**. Accordingly, the displacement of the atoms associated with the change of coordination is very different in both molecules; in particular the displacement of one fluorinated ligand would be impossible in **5** because it would result in unrealistic intermolecular F−F distances. In contrast, in **6** such steric congestion is not observed, and the coordination change is allowed.

Conclusion

From the connectivity point of view the system $Cu(hfac)_2$−IM-3Py should be able to form three dimensional networks. However, as is amply demonstrated, this goal was not reached. These complexes, however, exhibit very interesting magnetic properties, such as large ferromagnetic interactions and spin transitions.

To explain all the ferromagnetic couplings in compound **5** we propose an electron transfer mechanism (McConnell's second mechanism) which is consistent with the results of quantum chemical calculations. Although our understanding of this mechanism is poor, the presence of such large ferromagnetic interactions opens ways for designing high-spin species or molecular based magnetic materials.

Compound **6** displays a new type of spin transformation which was assigned to a change in coordination of the imino nitrogen from equatorial in a trigonal-bipyramidal geometry to axial in a square-planar pyramidal environment. However, this is only a *pseudo* spin transition since the ground state is high-spin in both cases, only the coupling constant changes from 213 to 8.6 cm^{-1}. In contrast, by analogy with **3**, the low-temperature transition which also exhibits hysteresis involves the nitroxyl oxygen coordination to the *endo*cyclic metal ion which switches from axial to equatorial.

Thus the two phases of $[Cu(hfac)_2]_4(IM\text{-}3Py)_2$ document the dependence of magnetic properties upon crystal packing and the possibility to design bistable spin-transition compounds based on copper(II) and nitroxide free radicals.

Acknowledgment. This work was supported by CEA, CNRS, and the European Community through the HCM (Grant CHRX CT 920080) and INTAS (Grant 94-3508) programs. L.Ö. is grateful to the Swedish Research Council for Engineering Sciences for a postdoctoral fellowship.

Supporting Information Available: Summary of crystal data (Table S1), positional parameters (Tables S2−S4), calculated position of the hydrogen atoms (Tables S5−S7), and complete listings of bond lengths (Tables S8−S10), bond angles (Tables S11−S13), and anisotropic thermal parameters (Tables S14−S16) (22 pages). Ordering information is given on any current masthead page.

IC951295Y